Electromagnetic Interrogation and the Doppler Shift Using the Method of Mappings

H.T. Banks, Shuhua Hu and W. Clayton Thompson
Center for Research in Scientific Computation
North Carolina State University
Raleigh, NC 27695-8212

December 11, 2009

Abstract

We consider the electromagnetic detection of hidden moving or oscillating conductive targets. The resulting mathematical problem involves computation of a Doppler shift for an electromagnetic wave reflecting from a moving interface. This entails solving Maxwell's equations on a domain changing in time. We employ the method of mappings to transform the problem to one of computing solutions of a Maxwell system with time dependent coefficients on a fixed reference domain. Thus we obtain a problem that is eminently tractable with finite element or finite difference time domain methods. Accuracy of numerical solutions is illustrated with computations for a number of different velocities for the moving interface.

AMS subject classifications: 35Q61,83C50,83C22,65M32.

Key Words: Electromagnetic Doppler shift, moving interfaces, method of mappings, finite elements.

1 Introduction

We consider the general problem of electromagnetic interrogation of a moving interface. In particular we are interested in the frequency shift (double Doppler shift) for an interrogating wave reflected from a moving conductive material target or interface. Such problems were first considered in 1905 by Einstein [8] in early work on relativity theory and have continued to be of interest in subsequent years [7, 9] especially in the context of modern radar technology (e.g., see [6, 9, 10] and the numerous references therein). In a number of applications the moving target may be one of *detection* in that the target is hidden or masked by a dielectric material (e.g., buried targets such as land mines, improvised explosive devices, etc., internal organs or implants or protheses, internal aircraft or automotive engine components). The targets of interest may be moving due to external disturbances (such as elastic waves as used in seismic exploration, acoustic waves as used in medical probes) or natural vibrations (e.g., rotating aircraft engine compressor blades, contracting/expanding arteries in compressed or normal blood circulation). In any case, for many such examples the mathematical problem is rather simply stated: one must analyze Maxwell's equations on a moving domain, i.e., a domain with moving boundaries or interfaces.

The classical approach often encountered in the literature (and described briefly below) makes use of the Lorentz transformation from relativity theory–see for example [6]. Related approaches (e.g., see [7, 9]) assume undamped time harmonic wave fields incident on a moving plane interface and determine reflection properties via boundary interface conditions. An approach that does not involve the Lorentz transformation includes that of [10] which is based on differentiation of interface conditions at moving boundaries and combining these with Maxwell's equations. This approach however still involves use of finite differences or finite elements on moving domains.

The ideas presented here in the context of the mathematical framework of [3] are based on the so-called *method of mappings* techniques frequently encountered in domain or shape optimization problems [11] that also have been used for example in thermal interrogation problems [4, 5] as well as in electromagnetic interrogation [3]. The ideas as illustrated here in a one dimensional setting are rather simply stated: one maps a constant (in time) coefficient partial differential equation (e.g., Maxwell's equations) given on a time changing or moving domain to a partial differential equation with time-dependent coefficients but on a fixed reference domain. The resulting problems are thus quite suitable for solution by finite difference or finite element numerical methods. This approach is not restricted to simple rectilinear movement of the interfaces or boundaries. The approach is simple, requires no relativistic transformations and can in principle, be used in interrogation problems for complex moving targets in higher dimensions when combined with perfectly matched layer (PML) formulations [1, 2]. Our primary requirement is that the moving interface or target be defined by an H^2 time dependent boundary. We describe the ideas in the context of an impulsive electromagnetic signal impinging normally on a vibrating conductive plane interface that is hidden by a dielectric layer such as soil or tissue.

2 General Case

We illustrate the basic ideas in the context of the framework developed in [3]. We formulate a mathematical model governing the electric field intensity of a polarized electromagnetic pulse emitted by an antenna as it propagates from air to a dielectric (we use parameters for soil here), partially reflects and partially transmits at the air/dielectric interface, propagates through the dielectric and then reflects from a perfectly conducting surface (the target), and propagates back to the air. We will consider the geometry shown in Figure 1. The positive z axis extends to the right in the figure; the air-soil interface is fixed at $z = 0$ while the target (assumed to be a perfect conductor) is mobile, with position given by $z_{10}(t)$ (assumed > 0). The left boundary of the domain (where we will place a source current) without loss of generality is assumed to be at $z = -1$.

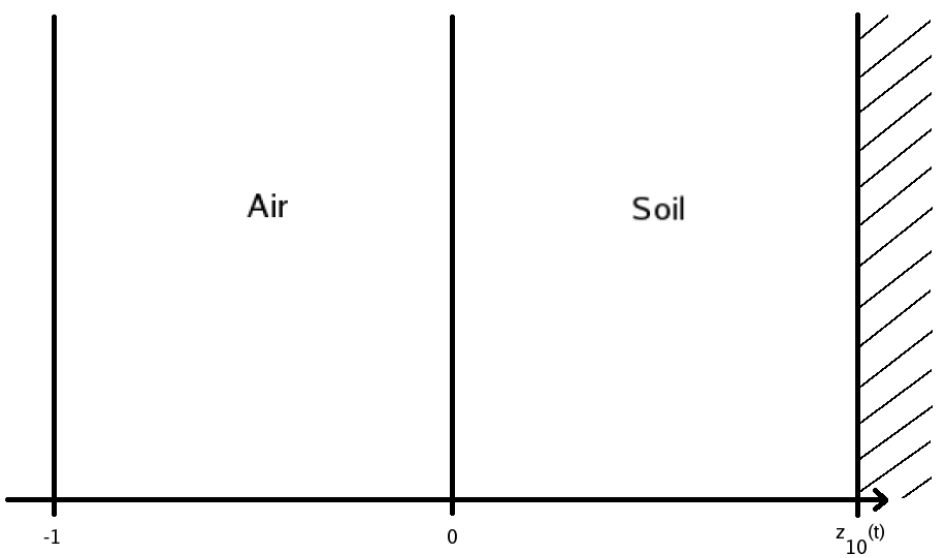

Figure 1: Geometry of the 1D mathematical model for EM interrogation.

With this geometry, we may now write the governing equation [3] for the electric field on the domain $z \in [-1, z_{10}(t)]$, $t \geq 0$. For $z \in [-1, 0]$, we have the standard Maxwell's equation

$$\frac{\partial^2 E(t,z)}{\partial t^2} - c^2 \frac{\partial^2 E(t,z)}{\partial z^2} = -\frac{1}{\epsilon_0} \frac{\partial J_s(t,z)}{\partial t}. \tag{1}$$

Here we do not distinguish air from a vacuum. For $z \in [0, z_{10}(t)]$, we have

$$\begin{aligned} \epsilon_r \frac{\partial^2 E(t,z)}{\partial t^2} &+ \frac{1}{\epsilon_0}\Big(\sigma(z) + g(0,z)\Big)\frac{\partial E(t,z)}{\partial t} \\ &+ \frac{1}{\epsilon_0}\left(\frac{\partial g(t,z)}{\partial t}E(0,z) + \int_0^t \frac{\partial g(t-s,z)}{\partial t}\frac{\partial E(s,z)}{\partial s}ds\right) \\ &- c^2\frac{\partial^2 E(t,z)}{\partial z^2} = -\frac{1}{\epsilon_0}\frac{\partial J_s(t,z)}{\partial t}. \end{aligned} \tag{2}$$

These equations have been adapted from [3, eqn (2.14)]; here $\epsilon_r = \dfrac{\epsilon}{\epsilon_0}$ is the relative permittivity of the dielectric, $\sigma(z)$ is the conductivity of soil, $g(t,z)$ is the polarization susceptibility kernel, and $J_s(t,z)$ is the source current. We make two simplifying assumptions. First, the soil is assumed to be uniform throughout, so that $\sigma(z) = \sigma$. Second, we assume that the source current is emitted from a point at the left boundary of the spatial domain and has the form

$$J_s(t,z) = \delta(z+1)j(t), \tag{3}$$

where $j(t)$ is a function to be specified and δ is the Dirac delta distribution with support at $\{0\}$.

We assume that the electric field intensity is initially zero and static so that the initial conditions are

$$\begin{aligned} E(0,z) &= 0 \\ \frac{\partial E}{\partial t}(0,z) &= 0, \end{aligned}$$

for $z \in [-1, z_{10}(t)]$. We assume that the target is a perfect conductor and that there is no reflection from the left boundary (absorbing boundary conditions). Thus the boundary conditions are

$$\left[\frac{1}{c}\frac{\partial E}{\partial t} - \frac{\partial E}{\partial z}\right]_{z=-1} = 0$$

$$E(t, z_{10}(t)) = 0.$$

For this problem the domain on which the equations hold $[-1, z_{10}(t)]$ is time-varying. Hence any direct numerical method invoked to solve the given equations on such a domain would be prohibitively expensive computationally. In order to overcome such a difficultly, we will employ the method of mappings [4, 5, 11] to transform the problem to one with a state variable defined on a constant domain $[-1, 1]$. The technique is in fact simply a change of variables for the system.

2.1 Method of Mappings

Given the function $z_{10}(t)$, we consider the change of variables $(t, z) \to (\tau, \zeta)$ defined by

$$\begin{aligned} \zeta(t,z) &= \begin{cases} z, & z \le 0 \\ \dfrac{z}{z_{10}(t)}, & z > 0 \end{cases} \\ \tau(t) &= t, \end{aligned}$$

with inverse transformation

$$\begin{aligned} z(\tau,\zeta) &= \begin{cases} \zeta, & \zeta \le 0 \\ \zeta z_{10}(\tau), & \zeta > 0 \end{cases} \\ t(\tau) &= \tau. \end{aligned}$$

It is easy to verify that the transformation is locally invertible provided $z_{10}(t) \neq 0$, which we have already assumed. Moreover, it maps the domain $[-1, z_{10}(t)]$ to the fixed reference domain $[-1, 1]$. We now undertake the task of transforming the original system (in $E(t, z)$ on $[-1, z_{10}(t)]$) into an equivalent system defined in terms of $\tilde{E}(\tau, \zeta)$ on $[-1, 1]$ where

$$E(t,z) = \tilde{E}(\tau(t), \zeta(t,z)).$$

For $z \le 0$, the transformation is simply a change of notation, and yields

$$\frac{\partial^2 \tilde{E}(\tau,\zeta)}{\partial \tau^2} - c^2 \frac{\partial^2 \tilde{E}(\tau,\zeta)}{\partial \zeta^2} = -\frac{\delta(\zeta+1)}{\epsilon_0} \frac{\partial j(\tau)}{\partial \tau}. \tag{4}$$

For $z > 0$, we invoke the chain rule for each of the derivatives appearing in (2). For the state variable, we have

$$\frac{\partial E}{\partial z} = \frac{\partial \tilde{E}}{\partial \zeta}\frac{\partial \zeta}{\partial z} = \frac{\partial \tilde{E}}{\partial \zeta}\frac{1}{z_{10}(t)}. \tag{5}$$

Continuing to the second derivative with respect to the state variable, we obtain

$$\frac{\partial^2 E}{\partial z^2} = \frac{\partial}{\partial z}\left[\frac{1}{z_{10}(t)}\frac{\partial \tilde{E}}{\partial \zeta}\right] = \frac{\partial}{\partial \zeta}\left[\frac{1}{z_{10}(t)}\frac{\partial \tilde{E}}{\partial \zeta}\right]\frac{\partial \zeta}{\partial z} = \frac{1}{z_{10}^2(t)}\frac{\partial^2 \tilde{E}}{\partial \zeta^2}. \tag{6}$$

For the time variable, we find

$$\begin{aligned} \frac{\partial E}{\partial t} &= \frac{\partial \tilde{E}}{\partial \tau}\frac{\partial \tau}{\partial t} + \frac{\partial \tilde{E}}{\partial \zeta}\frac{\partial \zeta}{\partial t} \\ &= \frac{\partial \tilde{E}}{\partial \tau} - \frac{\partial \tilde{E}}{\partial \zeta}\left(\frac{z}{z_{10}^2(t)}\frac{\partial z_{10}(t)}{\partial t}\right). \end{aligned} \tag{7}$$

Continuing for the second derivative, we have

$$
\begin{aligned}
\frac{\partial^2 E}{\partial t^2} &= \frac{\partial}{\partial t}\left[\frac{\partial \tilde{E}}{\partial \tau} - \frac{\partial \tilde{E}}{\partial \zeta}\left(\frac{z}{z_{10}^2(t)}\frac{\partial z_{10}(t)}{\partial t}\right)\right] \\
&= \frac{\partial}{\partial \tau}\left[\frac{\partial \tilde{E}}{\partial \tau}\right]\frac{\partial \tau}{\partial t} + \frac{\partial}{\partial \zeta}\left[\frac{\partial \tilde{E}}{\partial \tau}\right]\frac{\partial \zeta}{\partial t} - \frac{\partial}{\partial t}\left[\frac{\partial \tilde{E}}{\partial \zeta}\left(\frac{z}{z_{10}^2(t)}\frac{\partial z_{10}(t)}{\partial t}\right)\right] \\
&= \frac{\partial^2 \tilde{E}}{\partial \tau^2} - \frac{\partial^2 \tilde{E}}{\partial \zeta \partial \tau}\left(\frac{z}{z_{10}^2(t)}\frac{\partial z_{10}(t)}{\partial t}\right) - \frac{\partial \tilde{E}}{\partial \zeta}\frac{\partial}{\partial t}\left[\frac{z}{z_{10}^2(t)}\frac{\partial z_{10}(t)}{\partial t}\right] - \frac{z}{z_{10}^2(t)}\frac{\partial z_{10}(t)}{\partial t}\frac{\partial}{\partial t}\left[\frac{\partial \tilde{E}}{\partial \zeta}\right] \\
&= \frac{\partial^2 \tilde{E}}{\partial \tau^2} - \frac{\partial^2 \tilde{E}}{\partial \zeta \partial \tau}\left(\frac{z}{z_{10}^2(t)}\frac{\partial z_{10}(t)}{\partial t}\right) - \frac{\partial \tilde{E}}{\partial \zeta}\left(\frac{\partial z_{10}(t)}{\partial t}\frac{-2z}{z_{10}^3(t)}\frac{\partial z_{10}(t)}{\partial t} + \frac{z}{z_{10}^2(t)}\frac{\partial^2 z_{10}(t)}{\partial t^2}\right) \\
&\quad - \frac{z}{z_{10}^2(t)}\frac{\partial z_{10}(t)}{\partial t}\left(\frac{\partial}{\partial \tau}\left[\frac{\partial \tilde{E}}{\partial \zeta}\right]\frac{\partial \tau}{\partial t} + \frac{\partial}{\partial \zeta}\left[\frac{\partial \tilde{E}}{\partial \zeta}\right]\frac{\partial \zeta}{\partial t}\right) \\
&= \frac{\partial^2 \tilde{E}}{\partial \tau^2} - 2\frac{\partial^2 \tilde{E}}{\partial \zeta \partial \tau}\left(\frac{z}{z_{10}^2(t)}\frac{\partial z_{10}(t)}{\partial t}\right) + \frac{\partial \tilde{E}}{\partial \zeta}\left[\frac{2z}{z_{10}^3(t)}\left(\frac{\partial z_{10}(t)}{\partial t}\right)^2 - \frac{z}{z_{10}^2(t)}\frac{\partial^2 z_{10}(t)}{\partial t^2}\right] \\
&\quad + \frac{\partial^2 \tilde{E}}{\partial \zeta^2}\left(\frac{z}{z_{10}^2(t)}\frac{\partial z_{10}(t)}{\partial t}\right)^2. \qquad (8)
\end{aligned}
$$

Replacing the variables z and t where they appear in Equations (5) - (8) with $\zeta z_{10}(\tau)$ and τ respectively, we find

$$
\begin{aligned}
\frac{\partial E}{\partial t} &= \frac{\partial \tilde{E}}{\partial \tau} - \frac{\partial \tilde{E}}{\partial \zeta}\left(\frac{\zeta}{z_{10}(\tau)}\frac{\partial z_{10}(\tau)}{\partial \tau}\right) \qquad (9) \\
\frac{\partial^2 E}{\partial t^2} &= \frac{\partial^2 \tilde{E}}{\partial \tau^2} - 2\frac{\partial^2 \tilde{E}}{\partial \zeta \partial \tau}\left(\frac{\zeta}{z_{10}(\tau)}\frac{\partial z_{10}(\tau)}{\partial \tau}\right) + \frac{\partial \tilde{E}}{\partial \zeta}\left[\frac{2\zeta}{z_{10}^2(\tau)}\left(\frac{\partial z_{10}(\tau)}{\partial \tau}\right)^2 - \frac{\zeta}{z_{10}(\tau)}\frac{\partial^2 z_{10}(\tau)}{\partial \tau^2}\right] \\
&\quad + \frac{\partial^2 \tilde{E}}{\partial \zeta^2}\left(\frac{\zeta}{z_{10}(\tau)}\frac{\partial z_{10}(\tau)}{\partial \tau}\right)^2 \qquad (10) \\
\frac{\partial E}{\partial z} &= \frac{\partial \tilde{E}}{\partial \zeta}\frac{1}{z_{10}(\tau)} \qquad (11) \\
\frac{\partial^2 E}{\partial z^2} &= \frac{1}{z_{10}^2(\tau)}\frac{\partial^2 \tilde{E}}{\partial \zeta^2}. \qquad (12)
\end{aligned}
$$

We observe that $E(0,z) = \tilde{E}(\tau(0), \zeta(0,z)) = \tilde{E}(0,\zeta)$ for all z. We also need a means of treating the polarization kernel $g(t,z)$ in the original formulation. To this end we define $\tilde{g}$ via $g(t,z) = \tilde{g}(\tau(t), \zeta(t,z))$ or, equivalently, $\tilde{g}(\tau,\zeta) = g(t(\tau), z(\tau,\zeta))$. Also note that we need only

consider the transformation of the function g when $z > 0$. Thus

$$\begin{aligned}
\frac{\partial g}{\partial t} &= \frac{\partial \tilde{g}}{\partial \tau}\frac{\partial \tau}{\partial t} + \frac{\partial \tilde{g}}{\partial \zeta}\frac{\partial \zeta}{\partial t} \\
&= \frac{\partial \tilde{g}}{\partial \tau} - \frac{\partial \tilde{g}}{\partial \zeta}\left(\frac{z}{z_{10}^2(t)}\frac{\partial z_{10}(t)}{\partial t}\right) \\
&= \frac{\partial \tilde{g}}{\partial \tau} - \frac{\partial \tilde{g}}{\partial \zeta}\left(\frac{\zeta}{z_{10}(\tau)}\frac{\partial z_{10}(\tau)}{\partial \tau}\right).
\end{aligned} \tag{13}$$

We are finally ready to substitute these expressions (9)-(13) into (2) and obtain

$$\begin{aligned}
&\frac{\epsilon}{\epsilon_0}\left[\frac{\partial^2 \tilde{E}}{\partial \tau^2} - 2\frac{\partial^2 \tilde{E}}{\partial \zeta \partial \tau}\left(\frac{\zeta}{z_{10}(\tau)}\frac{\partial z_{10}(\tau)}{\partial \tau}\right) + \frac{\partial \tilde{E}}{\partial \zeta}\left(\frac{2\zeta}{z_{10}^2(\tau)}\left(\frac{\partial z_{10}(\tau)}{\partial \tau}\right)^2 - \frac{\zeta}{z_{10}(\tau)}\frac{\partial^2 z_{10}(\tau)}{\partial \tau^2}\right)\right. \\
&\quad \left. + \frac{\partial^2 \tilde{E}}{\partial \zeta^2}\left(\frac{\zeta}{z_{10}(\tau)}\frac{\partial z_{10}(\tau)}{\partial \tau}\right)^2\right] + \frac{1}{\epsilon_0}\Big(\sigma + \tilde{g}(0,\zeta)\Big)\left[\frac{\partial \tilde{E}}{\partial \tau} - \frac{\partial \tilde{E}}{\partial \zeta}\left(\frac{\zeta}{z_{10}(\tau)}\frac{\partial z_{10}(\tau)}{\partial \tau}\right)\right] \\
&\quad + \frac{1}{\epsilon_0}\int_0^\tau \left(\frac{\partial \tilde{g}(\tau - s,\zeta)}{\partial \tau} - \frac{\partial \tilde{g}(\tau - s,\zeta)}{\partial \zeta}\frac{\zeta}{z_{10}(\tau - s)}\frac{\partial z_{10}(\tau - s)}{\partial \tau}\right) \\
&\qquad \left(\frac{\partial \tilde{E}(s,\zeta)}{\partial s} - \frac{\partial \tilde{E}(s,\zeta)}{\partial \zeta}\left(\frac{\zeta}{z_{10}(s)}\frac{\partial z_{10}(s)}{\partial s}\right)\right) ds \\
&\quad + \frac{1}{\epsilon_0}\left(\frac{\partial \tilde{g}}{\partial \tau} - \frac{\partial \tilde{g}}{\partial \zeta}\frac{\zeta}{z_{10}(\tau)}\frac{\partial z_{10}(\tau)}{\partial \tau}\right)\tilde{E}(0,\zeta) - c^2\frac{1}{z_{10}^2(\tau)}\frac{\partial^2 \tilde{E}}{\partial \zeta^2} = 0,
\end{aligned} \tag{14}$$

for $\tau \geq 0$ and $\zeta \in [0,1]$. Observe that the right side of the equation is zero because the source current is zero in the given domain. Together with (4), (14) provides a piecewise set of equations for $\tilde{E}$. It follows trivially that the new initial conditions are

$$\begin{aligned}
\tilde{E}(0,\zeta) &= 0 \\
\frac{\partial}{\partial \tau}\tilde{E}(0,\zeta) &= 0,
\end{aligned} \tag{15}$$

and the boundary conditions are

$$\begin{aligned}
&\left[\frac{1}{c}\frac{\partial \tilde{E}}{\partial \tau} - \frac{\partial \tilde{E}}{\partial \zeta}\right]_{\zeta=-1} = 0 \\
&\tilde{E}(\tau,1) = 0.
\end{aligned} \tag{16}$$

Equations (4) and (14) - (16) completely describe $\tilde{E}(\tau,\zeta)$ for $\tau \geq 0$ and $\zeta \in [-1,1]$. These equations can be readily solved and the solution returned to the original coordinates to obtain the electric field intensity $E(t,z)$ on the time-varying domain $[-1, z_{10}(t)]$.

3 A Special Case: The Case without Dissipation

In order to validate and demonstrate the application of the method of mappings technique, we consider a simplified problem equivalent to that discussed by Van Bladel in [6, Sec 5.9]. We assume as in [6] a time-harmonic plane wave in a vacuum is normally incident on a perfect conductor which is moving with constant velocity parallel to the direction of wave propagation. Thus the need to consider dispersion or polarization in the soil is removed ($\sigma = 0, g(t, z) = 0$). The position of the target is $z_{10}(t) = v_z t + z_0$ where v_z is the velocity of the target and z_0 is its position at $t = 0$. We will also assume that the source current is sinusoidal in time, $j(t) = \sin(\omega t)$.

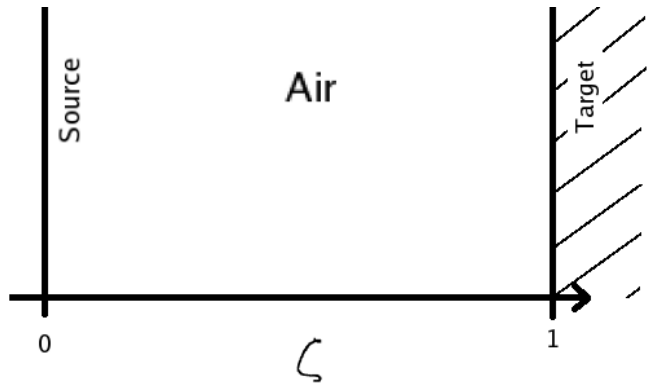

Figure 2: Geometry of the undamped problem in the ζ coordinate.

This problem is well-known from basic relativistic considerations (as shown in [6, Sec 5.9]) to produce a so-called "double Doppler shift", so that the frequency of the wave reflected from the conductor is

$$f_r = f_i \frac{1 - v_z/c}{1 + v_z/c}, \tag{17}$$

where f_i denotes the frequency of incident wave. The derivation is based on the Lorentz transformation from classical relativity theory. We now seek to use the method of mappings to recreate this result computationally and thus demonstrate the efficacy of the proposed method. For simplicity, we will only consider the electric field on the domain $z \in [0, z_{10}(t)]$ (the vacuum will not change the wave form, so moving the left boundary from $z = -1$ to $z = 0$ does not change the problem; the source current will thus be $J_s(t, z) = \delta(z)\sin(\omega t)$). After the appropriate change of variables, the new geometry for this special case is shown in Figure 2 and the governing equation is

$$\begin{aligned} \frac{\partial^2 \tilde{E}(\tau,\zeta)}{\partial \tau^2} &- 2\frac{\partial^2 \tilde{E}(\tau,\zeta)}{\partial \zeta \partial \tau}\left(\frac{v_z \zeta}{v_z \tau + z_0}\right) + \frac{\partial \tilde{E}(\tau,\zeta)}{\partial \zeta}\left[\frac{2v_z^2 \zeta}{(v_z\tau + z_0)^2}\right] \\ &- \frac{\partial^2 \tilde{E}(\tau,\zeta)}{\partial \zeta^2}\left(\frac{c^2 - v_z^2\zeta^2}{(v_z\tau + z_0)^2}\right) = -\frac{\omega}{\epsilon_0}\delta(\zeta z_{10}(\tau))\cos(\omega\tau), \end{aligned} \tag{18}$$

with boundary conditions

$$\left[\frac{1}{c}\frac{\partial \tilde{E}}{\partial \tau} - \frac{1}{z_{10}(\tau)}\frac{\partial \tilde{E}}{\partial \zeta}\right]_{\zeta=0} = 0 \qquad (19)$$
$$\tilde{E}(\tau, 1) = 0.$$

The initial conditions are still given by (15).

3.1 Weak/Variational Formulation

We next proceed to write (18) and (19) into variational form in preparation for the introduction of numerical approximations. Define

$$\alpha(\tau,\zeta) = \frac{2v_z\zeta}{v_z\tau + z_0}, \quad \beta(\tau,\zeta) = \frac{2v_z^2\zeta}{(v_z\tau + z_0)^2}, \quad \gamma(\tau,\zeta) = \frac{c^2 - v_z^2\zeta^2}{(v_z\tau + z_0)^2}.$$

Let $\langle\cdot,\cdot\rangle$ be the standard $L^2(0,1)$ inner product and let $\phi \in H_R^1(0,1) \equiv \{\phi \in H^1(0,1) | \phi(1) = 0\}$. Then

$$\begin{aligned}\left\langle \frac{\partial^2 \tilde{E}(\tau,\cdot)}{\partial \tau^2}, \phi \right\rangle &- \left\langle \alpha(\tau,\cdot)\frac{\partial^2 \tilde{E}(\tau,\cdot)}{\partial \tau \partial \zeta}, \phi \right\rangle + \left\langle \beta(\tau,\cdot)\frac{\partial \tilde{E}(\tau,\cdot)}{\partial \zeta}, \phi \right\rangle \\ &- \left\langle \gamma(\tau,\cdot)\frac{\partial^2 \tilde{E}(\tau,\cdot)}{\partial \zeta^2}, \phi \right\rangle = \left\langle -\frac{\omega}{\epsilon_0}\delta(\zeta z_{10}(\tau))\cos(\omega\tau), \phi \right\rangle.\end{aligned} \qquad (20)$$

We then use integration by parts on the fourth term of (20). In our subsequent discussions, we let $(\,'\,)$ be the $\frac{\partial}{\partial \zeta}$ derivative and $(\dot{\,})$ be the $\frac{\partial}{\partial \tau}$ derivative: we have

$$\begin{aligned}&\left\langle \gamma(\tau,\cdot)\frac{\partial^2 \tilde{E}(\tau,\cdot)}{\partial \zeta^2}, \phi \right\rangle \\ &\quad = \gamma(\tau,\zeta)\phi(\zeta)\frac{\partial \tilde{E}(\tau,\zeta)}{\partial \zeta}\bigg|_0^1 - \int_0^1 \frac{\partial \tilde{E}(\tau,\zeta)}{\partial \zeta}(\gamma(\tau,\zeta)\phi'(\zeta) + \gamma'(\tau,\zeta)\phi(\zeta))d\zeta \\ &\quad = -\gamma(\tau,0)\phi(0)\frac{\partial \tilde{E}(\tau,0)}{\partial \zeta} - \left\langle \frac{\partial \tilde{E}}{\partial \zeta}, \gamma(\tau,\cdot)\phi' + \gamma'(\tau,\cdot)\phi \right\rangle.\end{aligned} \qquad (21)$$

For the source current term, we find

$$\left\langle -\frac{\omega}{\epsilon_0}\delta(\zeta z_{10}(\tau))\cos(\omega\tau), \phi \right\rangle = -\frac{\omega}{\epsilon_0 z_{10}(\tau)}\cos(\omega\tau)\phi(0). \qquad (22)$$

Substituting (21) and (22) into (20), we obtain

$$\left\langle \frac{\partial^2 \tilde{E}(\tau,\cdot)}{\partial \tau^2}, \phi \right\rangle - \left\langle \alpha(\tau,\cdot)\frac{\partial^2 \tilde{E}(\tau,\cdot)}{\partial \tau \partial \zeta}, \phi \right\rangle + \left\langle \beta(\tau,\cdot)\frac{\partial \tilde{E}(\tau,\cdot)}{\partial \zeta}, \phi \right\rangle + \gamma(\tau,0)\phi(0)\frac{\partial \tilde{E}(\tau,0)}{\partial \zeta}$$
$$+ \left\langle \frac{\partial \tilde{E}(\tau,\cdot)}{\partial \zeta}, \gamma(\tau,\cdot)\phi' + \gamma'(\tau,\cdot)\phi \right\rangle = -\frac{\omega}{\epsilon_0 z_{10}(\tau)}\cos(\omega\tau)\phi(0). \tag{23}$$

Now observe that

$$\begin{aligned} \gamma(\tau,0)\phi(0)\frac{\partial \tilde{E}(\tau,0)}{\partial \zeta} &- \frac{1}{c}\gamma(\tau,0)\phi(0)z_{10}(\tau)\frac{\partial \tilde{E}(\tau,0)}{\partial \tau} \\ &= -\gamma(\tau,0)\phi(0)z_{10}(\tau)\left[\frac{1}{c}\frac{\partial \tilde{E}}{\partial \tau} - \frac{1}{z_{10}(\tau)}\frac{\partial \tilde{E}}{\partial \zeta}\right]_{\zeta=0} = 0 \end{aligned}$$

by the boundary condition at $\zeta = 0$. Thus the resulting variational form is

$$\begin{aligned} &\left\langle \frac{\partial^2 \tilde{E}(\tau,\cdot)}{\partial \tau^2}, \phi \right\rangle - \left\langle \alpha(\tau,\cdot)\frac{\partial^2 \tilde{E}(\tau,\cdot)}{\partial \tau \partial \zeta}, \phi \right\rangle + \left\langle \beta(\tau,\cdot)\frac{\partial \tilde{E}(\tau,\cdot)}{\partial \zeta}, \phi \right\rangle \\ &+\frac{1}{c}\gamma(\tau,0)\phi(0)z_{10}(\tau)\frac{\partial \tilde{E}(\tau,0)}{\partial \tau} + \left\langle \frac{\partial \tilde{E}(\tau,\cdot)}{\partial \zeta}, \gamma(\tau,\cdot)\phi' + \gamma'(\tau,\cdot)\phi \right\rangle \\ &= -\frac{\omega}{\epsilon_0 z_{10}(\tau)}\cos(\omega\tau)\phi(0). \end{aligned} \tag{24}$$

The functions $\alpha(\tau,\zeta)$, $\beta(\tau,\zeta)$, and $\gamma(\tau,\zeta)$ are real valued and the weak derivative γ' can be easily computed analytically.

3.2 Finite Elements Method

To solve (24), we use first order finite elements methods (FEM). We assume that the ζ domain has been partitioned into an evenly spaced grid (step size h) with nodes ζ_k, $k = 0, \ldots, N$ ($\zeta_k = hk$). We then define the 'hat' functions (piecewise linear splines)

$$\phi_0(\zeta) = \begin{cases} \dfrac{\zeta_1 - \zeta}{h}, & \zeta \le \zeta_1 \\ 0, & otherwise \end{cases},$$

$$\phi_i(\zeta) = \begin{cases} \dfrac{\zeta - \zeta_{i-1}}{h}, & \zeta_{i-1} \le \zeta \le \zeta_i \\ \dfrac{\zeta_{i+1} - \zeta}{h}, & \zeta_i \le \zeta \le \zeta_{i+1} \\ 0, & otherwise \end{cases} \qquad i = 1, \ldots, N-1.$$

Following standard FEM technique, we assume that the solution to (24) can be approximated as

$$\tilde{E}(\tau,\zeta) \approx \tilde{E}^N(\tau,\zeta) \equiv \sum_{i=0}^{N-1} w_i(\tau)\phi_i(\zeta),$$

where the N coefficient functions $w_i(\tau)$ are now the unknowns to be determined via (24). With these substitutions into equation (24), we now have an infinite number of equations in N unknowns (recall that (24) must hold for all $\phi \in H_R^1(0,1)$). In order to form a uniquely determinable system of equations, we let $\phi(\zeta) = \phi_j(\zeta)$, $j = 0,\ldots,N-1$, in turn. Then for each $j = 0,\ldots,N-1$, we must have

$$\begin{aligned}\sum_{i=0}^{N-1} \ddot{w}_i(\tau)\langle\phi_i,\phi_j\rangle \quad &- \quad \sum_{i=0}^{N-1} \dot{w}_i(\tau)\langle\alpha(\tau,\cdot)\phi_i',\phi_j\rangle + \sum_{i=0}^{N-1} w_i(\tau)\langle\beta(\tau,\cdot)\phi_i',\phi_j\rangle \\ &+ \quad \frac{1}{c}\gamma(\tau,0)\phi_j(0)z_{10}(\tau)\dot{w}_0(\tau) + \sum_{i=0}^{N-1} w_i(\tau)\langle\phi_i',\gamma(\tau,\cdot)\phi_j'\rangle \\ &+ \quad \sum_{i=0}^{N-1} w_i(\tau)\langle\phi_i',\gamma'(\tau,\cdot)\phi_j\rangle = -\frac{\omega}{\epsilon_0 z_{10}(\tau)}\cos(\omega\tau)\phi_j(0).\end{aligned} \tag{25}$$

This constitutes N equations for the N unknowns $w_i,\ i = 0,1,\ldots,N-1$. It is also useful to compute the following:

$$\langle\phi_i,\phi_j\rangle = \begin{cases} h/3, & i=j=0 \\ 2h/3, & i=j\neq 0 \\ h/6, & |i-j|=1 \\ 0, & otherwise \end{cases} \tag{26}$$

$$\langle\alpha(\tau,\cdot)\phi_i',\phi_j\rangle = \begin{cases} \dfrac{-v_z h}{3(v_z\tau+z_0)}, & i=j=0 \\ \dfrac{-2v_z h}{3(v_z\tau+z_0)}, & i=j\neq 0 \\ \dfrac{v_z(3i-2)h}{3(v_z\tau+z_0)}, & i=j+1 \\ \dfrac{-v_z(3i+2)h}{3(v_z\tau+z_0)}, & i=j-1 \\ 0, & otherwise \end{cases} \tag{27}$$

$$\langle\beta(\tau,\cdot)\phi_i',\phi_j\rangle = \begin{cases} \dfrac{-v_z^2 h}{3(v_z\tau+z_0)^2}, & i=j=0 \\ \dfrac{-2v_z^2 h}{3(v_z\tau+z_0)^2}, & i=j\neq 0 \\ \dfrac{v_z^2(3i-2)h}{3(v_z\tau+z_0)^2}, & i=j+1 \\ \dfrac{-v_z^2(3i+2)h}{3(v_z\tau+z_0)^2}, & i=j-1 \\ 0, & otherwise \end{cases} \tag{28}$$

$$\langle \phi_i', \gamma(\tau,\cdot)\phi_j' \rangle = \begin{cases} \dfrac{3c^2 - v_z^2 h^2}{3h(v_z\tau + z_0)^2}, & i = j = 0 \\ \dfrac{6c^2 - 2v_z^2 h^2(3i^2+1)}{3h(v_z\tau + z_0)^2}, & i = j \neq 0 \\ \dfrac{v_z^2 h^2(3i^2 - 3i + 1) - 3c^2}{3h(v_z\tau + z_0)^2}, & i = j+1 \\ \dfrac{v_z^2 h^2(3i^2 + 3i + 1) - 3c^2}{3h(v_z\tau + z_0)^2}, & i = j-1 \\ 0, & otherwise \end{cases}, \tag{29}$$

$$\langle \phi_i', \gamma'(\tau,\cdot)\phi_j \rangle = \begin{cases} \dfrac{v_z^2 h}{3(v_z\tau + z_0)^2}, & i = j = 0 \\ \dfrac{2v_z^2 h}{3(v_z\tau + z_0)^2}, & i = j \neq 0 \\ \dfrac{-v_z^2 h(3i-2)}{3(v_z\tau + z_0)^2}, & i = j+1 \\ \dfrac{v_z^2 h(3i+2)}{3(v_z\tau + z_0)^2}, & i = j-1 \\ 0, & otherwise \end{cases}. \tag{30}$$

Let $\boldsymbol{w}^N(\tau) = (w_0(\tau), w_1(\tau), \ldots, w_{N-1}(\tau))^T$. Then it follows that we can write (25) as a vector system with N equations in N variables

$$M\ddot{\boldsymbol{w}}^N(\tau) + \left(\frac{c}{v_z\tau + z_0}\mathbf{e}\mathbf{e}^T - C(\tau)\right)\dot{\boldsymbol{w}}^N(\tau) + (K_1(\tau) + K_2(\tau) + K_3(\tau))\boldsymbol{w}^N(\tau) = F(\tau), \tag{31}$$

where the (i,j)th element of M, C, K_1, K_2, and K_3 are defined in (26), (27), (28), (29) and (30), respectively, $\mathbf{e}$ is a N-dimensional column vector with a one as its first component and zeros otherwise, and $F(\tau)$ is a N-dimensional column vector given by

$$F(\tau) = \left(-\frac{\omega}{\epsilon_0 z_{10}(\tau)}\cos(\omega\tau), 0, 0, \ldots, 0\right)^T.$$

Thus (31) is a vector ordinary differential equation for the vector coefficient function $\boldsymbol{w}^N$ which can readily be solved numerically.

3.3 Computational Results

We first present results at *high velocity* to clearly demonstrate the accuracy of the method of mappings compared with that of classical electromagnetic Doppler shift computations. In carrying out the computations, we assume $z_0 = 2$. The electromagnetic source is truncated at $t = t^* = 4\pi/\omega$ so that only two sinusoidal pulses are emitted and reflected (this makes the determination of the periods of the incident and reflected waves easier to measure by limiting interference between the waves). That is, $j(t) = \sin(\omega t)I_{[0,t^*]}$ where I is the indicator function.

The following notation will be used throughout the remainder of this presentation: $f_{i,anl}$ denotes the frequency of the incident wave with which we interrogate the system (we use 1e+9 Hz in all calculations here), $f_{i,sim}$ is the corresponding frequency obtained by simulation. Similarly, we use $f_{r,anl}$ and $f_{r,sim}$ to represent the frequency of reflected waves obtained by using the Van Bladel formula (17) and simulation, respectively. Then the frequency shift obtained by the Van Bladel formula and simulation are calculated by

$$\Delta f_{anl} = |f_{i,anl} - f_{r,anl}|, \quad \text{and} \quad \Delta f_{sim} = |f_{i,sim} - f_{r,sim}|,$$

respectively. The relative error Rel_i for the incident wave is calculated by

$$\text{Rel}_i = 100\frac{|f_{i,anl} - f_{i,sim}|}{f_{i,anl}}.$$

Similarly, the relative error for the reflected wave and for the frequency shift are obtained by

$$\text{Rel}_r = 100\frac{|f_{r,anl} - f_{r,sim}|}{f_{r,anl}}, \quad \text{and} \quad \text{Rel}_s = 100\frac{|\Delta f_{anl} - \Delta f_{sim}|}{\Delta f_{anl}},$$

respectively.

In Figure 3, the magnitude of the electric field is shown as a function of time at a chosen value of z ($z = 0.3$), where the results are obtained with $v_z = 3\times10^3$ and $N = 16384$. In the top graph, the incident wave moves past $z = 0.3$ followed at some time later by the reflected wave. These two waves are magnified in the lower two graphs. Even though the electric field E has discontinuous derivative (w.r.t z) at the leading edges of the waves, numerical Gibbs type oscillations at these leading edges are resolved by using sufficiently large values of N (see [3] for discussions). The data displayed in the graph can be used to estimate the period (and hence the frequency) of the waves as shown in the figure. Using this data, the estimated frequency of the incident wave is $f_{i,sim} = 999.999$MHz, and the relative error for incident wave is $\text{Rel}_i \approx 6.21 \times 10^{-6}\%$ (see Table 5). The estimated frequency of the reflected wave is $f_{r,sim} \approx 999.978$MHz with the relative error Rel_r being around $1.93 \times 10^{-4}\%$. The estimated frequency shift is $\Delta f_{sim} \approx .02187$MHz with relative error Rel_s being around 8.56%.

To see the effect of the values of v_z and N on the accuracy of the obtained frequency shift, we illustrated the results for $f_{i,anl}$, $f_{i,sim}$, $f_{r,anl}$, $f_{r,sim}$, Δf_{anl}, Δf_{sim}, Rel_i, Rel_r and Rel_s obtained by using different target velocity v_z (varied from 3×10^7 to 3×10^3) as well as different number N of spline functions (varied from 256 to 16384) in Tables 1-5. From these tables we can see that the relative error for the reflected wave (Rel_r) decreases as N increases. In addition, the frequency of reflected wave obtained by simulation ($f_{r,sim}$) is very close to that obtained by the Van Bladel formula ($f_{r,anl}$) for all the N's and velocities that we have tried. For example, even with $N = 256$, the relative error for the reflected wave is within 0.7% at the various velocities.

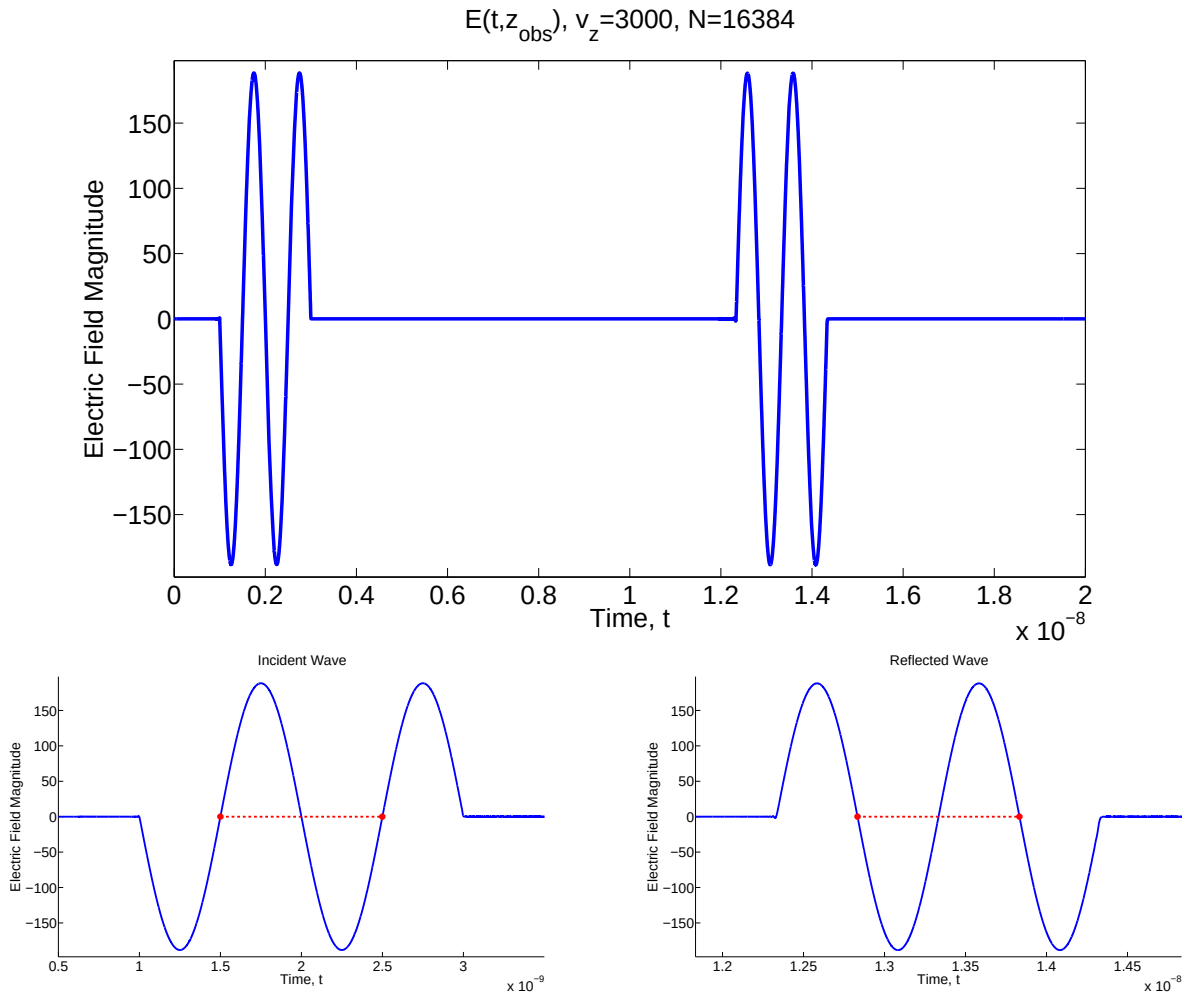

Figure 3: Electric field magnitude at $z = 0.3$ as a function of time. The incident and reflected waves are both visible in the top graphic and are magnified in the bottom graphics. The underlying data can be used to estimate the periods of the waves, and hence their frequencies.

We also observed that the relative error for the frequency shift (Rel_s) decreases as N increases. However, with the same number of spline functions used, the relative error for the frequency shift (Rel_s) increases as the velocity v_z decreases, and the ratio of relative errors obtained is roughly inversely proportional to the ratio of velocities used. For example, with $N = 256$, the relative error of frequency shift with $v_z = 3e + 7\ m/s$ is around 3.119% (see Table 1), while the relative error of frequency shift with $v_z = 3e{+}6\ m/s$ is about 30.828% (see Table 2). This is because with the same N we have roughly the same resolution for the estimated frequencies of the incident and reflected waves, but the frequency shift decreases roughly in the same proportion as the velocity decreases. Hence, in order to have the same order of accuracy for frequency shift, one requires relative errors Rel_i and Rel_r smaller (by increasing the number of spline functions) as the

N		Incident wave	Reflected wave	Frequency shift
256	Frequency (Hz)	1.000121e+09	8.126322e+08	1.874889e+08
	Relative error (%)	1.211039e-02	6.782885e-01	3.118905e+00
512	Frequency (Hz)	1.000019e+09	8.155310e+08	1.844879e+08
	Relative error (%)	1.893419e-03	3.239856e-01	1.468349e+00
1024	Frequency (Hz)	9.999963e+08	8.177672e+08	1.822291e+08
	Relative error (%)	3.688152e-04	5.067185e-02	2.259949e-01
2048	Frequency (Hz)	1.000000e+09	8.184683e+08	1.815318e+08
	Relative error (%)	9.301384e-06	3.501080e-02	1.574975e-01
4096	Frequency (Hz)	9.999982e+08	8.180549e+08	1.819433e+08
	Relative error (%)	1.757703e-04	1.551259e-02	6.883992e-02
8192	Frequency (Hz)	9.999995e+08	8.181673e+08	1.818322e+08
	Relative error (%)	4.974886e-05	1.771110e-03	7.696376e-03
16384	Frequency (Hz)	1.000000e+09	8.181951e+08	1.818050e+08
	Relative error (%)	1.137230e-05	1.622042e-03	7.236642e-03
Van Bladel	Frequency (Hz)	1.000000e+09	8.181818e+08	1.818182e+08

Table 1: Results are obtained with $v_z = 3e + 7\ m/s$.

N		Incident wave	Reflected wave	Frequency shift
256	Frequency (Hz)	1.000011e+09	9.741044e+08	2.590645e+07
	Relative error (%)	1.083320e-03	6.216740e-01	3.082757e+01
512	Frequency (Hz)	1.000008e+09	9.789757e+08	2.103247e+07
	Relative error (%)	8.133255e-04	1.247048e-01	6.213959e+00
1024	Frequency (Hz)	1.000011e+09	9.810234e+08	1.898768e+07
	Relative error (%)	1.105998e-03	8.420359e-02	4.112225e+00
2048	Frequency (Hz)	1.000001e+09	9.798446e+08	2.015662e+07
	Relative error (%)	1.217442e-04	3.605618e-02	1.790929e+00
4096	Frequency (Hz)	1.000001e+09	9.800881e+08	1.991244e+07
	Relative error (%)	5.665388e-05	1.121088e-02	5.577997e-01
8192	Frequency (Hz)	1.000000e+09	9.801511e+08	1.984910e+07
	Relative error (%)	2.404050e-05	4.782805e-03	2.379629e-01
16384	Frequency (Hz)	1.000000e+09	9.801814e+08	1.981870e+07
	Relative error (%)	9.234616e-06	1.695973e-03	8.441702e-02
Van Bladel	Frequency (Hz)	1.000000e+09	9.801980e+08	1.980198e+07

Table 2: Results are obtained with $v_z = 3e + 6\ m/s$.

velocity decreases, even though $f_{r,sim}$ is already very close to the true value $f_{r,anl}$. This means that increased computational times and large memory requirements are required for smaller

N		Incident wave	Reflected wave	Frequency shift
256	Frequency (Hz)	1.000015e+09	9.915929e+08	8.422482e+06
	Relative error (%)	1.538420e-03	6.421927e-01	3.215452e+02
512	Frequency (Hz)	1.000017e+09	9.969054e+08	3.111440e+06
	Relative error (%)	1.682554e-03	1.098808e-01	5.572758e+01
1024	Frequency (Hz)	9.999983e+08	9.987907e+08	1.207639e+06
	Relative error (%)	1.685845e-04	7.902563e-02	3.955768e+01
2048	Frequency (Hz)	9.999965e+08	9.976733e+08	2.323195e+06
	Relative error (%)	3.536314e-04	3.293870e-02	1.627589e+01
4096	Frequency (Hz)	9.999984e+08	9.978469e+08	2.151500e+06
	Relative error (%)	1.574369e-04	1.553830e-02	7.682585e+00
8192	Frequency (Hz)	1.000000e+09	9.979663e+08	2.033657e+06
	Relative error (%)	9.115630e-07	3.573588e-03	1.784551e+00
16384	Frequency (Hz)	9.999997e+08	9.979980e+08	2.001690e+06
	Relative error (%)	3.121940e-00	4.008098e-04	1.845792e-01
Van Bladel	Frequency (Hz)	1.000000e+09	9.980020e+08	1.998002e+06

Table 3: Results are obtained with $v_z = 3e + 5\ m/s$.

N		Incident wave	Reflected wave	Frequency shift
256	Frequency (Hz)	1.000015e+09	9.933595e+08	6.655791e+06
	Relative error (%)	1.528581e-03	6.441814e-01	3.228228e+03
512	Frequency (Hz)	1.000017e+09	9.987374e+08	1.279175e+06
	Relative error (%)	1.661426e-03	1.062793e-01	5.396515e+02
1024	Frequency (Hz)	9.999981e+08	1.000582e+09	5.837657e+05
	Relative error (%)	1.865923e-04	7.820362e-02	1.919120e+02
2048	Frequency (Hz)	9.999973e+08	9.994617e+08	5.355922e+05
	Relative error (%)	2.725828e-04	3.384057e-02	1.678229e+02
4096	Frequency (Hz)	9.999993e+08	9.996484e+08	3.508599e+05
	Relative error (%)	7.140187e-05	1.516242e-02	7.544748e+01
8192	Frequency (Hz)	1.000000e+09	9.997639e+08	2.362211e+05
	Relative error (%)	1.213681e-05	3.612699e-03	1.812238e+01
16384	Frequency (Hz)	1.000000e+09	9.997977e+08	2.023030e+05
	Relative error (%)	3.711939e-06	2.360541e-04	1.161591e+00
Van Bladel	Frequency (Hz)	1.000000e+09	9.998000e+08	1.999800e+05

Table 4: Results are obtained with $v_z = 3e + 4\ m/s$.

velocities. For example, we only reduce the relative error in computed frequency shift (Rel_s) at velocities $v_z = 3e + 4\ m/s$ to around 75% with $N = 4096$, but for $N = 16384$ we can attain an

N		Incident wave	Reflected wave	Frequency shift
256	Frequency (Hz)	1.000015e+09	9.935310e+08	6.484262e+06
	Relative error (%)	1.526850e-03	6.449122e-01	3.232163e+04
512	Frequency (Hz)	1.000017e+09	9.989324e+08	1.084166e+06
	Relative error (%)	1.658583e-03	1.047601e-01	5.320885e+03
1024	Frequency (Hz)	9.999981e+08	1.000759e+09	7.610668e+05
	Relative error (%)	1.874295e-04	7.792079e-02	3.705372e+03
2048	Frequency (Hz)	9.999974e+08	9.996446e+08	3.527469e+05
	Relative error (%)	2.636166e-04	3.353899e-02	1.663752e+03
4096	Frequency (Hz)	9.999994e+08	9.998301e+08	1.693245e+05
	Relative error (%)	6.250510e-05	1.499528e-02	7.466310e+02
8192	Frequency (Hz)	1.000000e+09	9.999437e+08	5.639095e+04
	Relative error (%)	6.864313e-06	3.632324e-03	1.819576e+02
16384	Frequency (Hz)	9.999999e+08	9.999781e+08	2.187183e+04
	Relative error (%)	6.212735e-06	1.934194e-04	8.559082e+00
Van Bladel	Frequency (Hz)	1.000000e+09	9.999800e+08	1.999980e+04

Table 5: Results are obtained with $v_z = 3e + 3\ m/s$.

accuracy of 1% relative error at this velocity. For $v_z = 3e + 3\ m/s$ we can bring down Rel_s to approximately 8.5% with $N = 16384$.

4 Concluding Remarks

In the above discussions we have presented an approach to computation of frequency shifts for propagating electromagnetic waves reflected from a moving perfectly conducting target hidden by a dielectric layer. The approach relies on direct solution to the Maxwell system with general polarization mechanisms for dispersion in response to general impulsive inputs from an antenna source. The ideas are illustrated with theoretical formulation and computations in a one dimensional setting. One can readily extend the ideas to problems in which target interface and air/dielectric interface are both moving. The formulation can also be extended in principle to 2-D and 3-D geometries using ideas in [1]. The approach does not depend on time harmonic incident wave assumptions nor any relativistic transformations. It allows general motions including periodic and non-periodic oscillations. The ideas are currently being used in development of detection systems for buried targets.

Acknowledgements

This research was supported in part by the Air Force Office of Scientific Research under grant number FA9550-09-1-0226. The authors are grateful to Dr. Richard Albanese for encouragement,

suggestions and constructive comments related to the efforts reported on herein.

References

[1] H.T. Banks and V. A. Bokil, Parameter identification for dispersive dielectrics using pulsed microwave interrogating signals and acoustic wave induced reflections in two and three dimensions, CRSC-TR04-27, July, 2004; Revised version appeared as A computational and statistical framework for multidimensional domain acoustoptic material interrogation, *Quart. Applied Math.*, **63** (2005), 156–200.

[2] H.T. Banks and B. L. Browning, Time domain electromagnetic scattering using finite elements and perfectly matched layers, CRSC-TR02-23, July, 2002; Revised, June 2003; *Comp. Meth. Appl. Mech. Engr.*, **194** (2005), 149–168.

[3] H.T. Banks, M.W. Buksas and T. Lin,*Electromagnetic Material Interrogation Using Conductive Interfaces and Acoustic Wavefronts*, SIAM Frontiers in Applied Mathematics, **FR21**, SIAM, Philadelphia, PA (2000).

[4] H.T. Banks and F. Kojima, Boundary shape identification problems in two dimensional domains related to thermal testing of materials, LCDS/CSS Rep. 88-6, April, 1988; *Quart. Appl. Math.*, **47** (1989), 273–293.

[5] H.T. Banks, F. Kojima and W.P. Winfree, Boundary estimation problems arising in thermal tomography, CAMS Tech Rep. 89-6, University of Southern California; *Inverse Problems*, **6** (1990), 897–921.

[6] J. Van Bladel, *Relativity and Engineering*, Springer Series in Electrodynamics **15**, Springer: Berlin Heidlberg New York Tokyo (1984).

[7] J. Cooper, Scattering of electromagnetic fields by a moving boundary: The one-dimensional case, *IEEE Trans. Antennas and Propagation,* **AP-28** (1980), 791–795.

[8] A. Einstein, Zur elektrodynamik bewegter korperll, *Ann. Phys. (Leipzig)*, **17** (1905), 891–921.

[9] J.E. Gray, The Doppler spectrum for accelerating objects, *Proc. IEEE 1990 International Radar Conference*, Arlington, VA, May 7-10, 1990, Record (A91-25401 09-32), Institute of Electrical and Electronics Engineers, Inc., New York, 1990, p. 385–390.

[10] F. Harfoush, A. Taflove and G. Kriegsmann, Numerical implementation of relativistic electromagnetic boundary conditions in a laboratory-frame grid, *J. Comp. Physics*, **89** (1990), 80–94.

[11] O. Pironneau, *Optimal Shape Design for Elliptic Systems*, Springer-Verlag, New York, 1983.